

# Near-zero Radiation Induced Attenuation in Nested Anti-resonant Nodeless Hollow-core Fibers at 1550 nm

Sacha E. R. Medaer<sup>1,2</sup>, Diego Di Francesca<sup>1</sup>, Eric Numkam Fokoua<sup>3</sup>, Francesco Poletti<sup>3</sup>, Daniel Ricci<sup>1</sup>, Bernhard Schmauss<sup>2</sup>, Austin Taranta<sup>3</sup>, Iacopo Toccafondo<sup>1</sup>

1. CERN, European Organization for Nuclear Research, CH-1211 Geneva, Switzerland

2. Friedrich-Alexander University Erlangen Nürnberg, 91058 Erlangen, Germany

3. Optoelectronics Research Centre, University of Southampton, SO17 1BJ Southampton, UK  
[sacha.medaer@cern.ch](mailto:sacha.medaer@cern.ch), [daniel.ricci@cern.ch](mailto:daniel.ricci@cern.ch)

**Abstract:** The first nested anti-resonant hollow-core fiber radiation study is reported. A record near-zero radiation induced attenuation is observed under  $\gamma$ -rays and X-rays. These results open new possibilities for fiber-based applications in radiation environments. © 2022 The Author(s)

## 1. Introduction

Conventional solid-core fibers show an increase of optical attenuation when exposed to ionizing radiation. This phenomenon is called radiation induced attenuation (RIA). It can impair or even prevent fiber-based optical communication and optical sensing in facilities exposed to high levels of ionizing radiation, such as around nuclear reactors or in nuclear decommissioning sites, near high-energy physics experiments, as well as aboard spacecrafts or satellites. The strength of the RIA depends on many fiber-related parameters and on irradiation conditions [1]. The total ionizing dose (TID) is commonly expressed in gray (Gy) and refers to the quantity of energy deposited in the considered material per unit of mass (1 Gy = 1 J/kg). The TID values of fiber-based systems in radiation environment can range from 10 kGy for space applications to several MGy in nuclear facilities and high-energy physics experiments such as at CERN or ITER [2]. At these extreme doses, even the state-of-the-art radiation resistant fibers do eventually become opaque and need replacement, creating the need for an alternative solution.

In solid-core single mode fibers (SMF), light guidance relies on total internal reflection, where the refractive index of the core must be higher than that of the cladding. Unlike SMF, light guidance in hollow-core fibers (HCF) relies on a silica microstructured geometry to confine the optical modes in the core, which allows the refractive index of the core to be close to unity. The two main types of HCFs are photonic bandgap fibers (PBGF) and anti-resonant fibers (ARF). The former relies on a photonic bandgap for light guidance whereas the latter relies on anti-resonance and anti-coupling. Compared to SMFs, HCFs demonstrated low optical nonlinearity, low chromatic dispersion, and low Rayleigh scattering, as well as a near-vacuum latency. Fiber topology such as the double nested anti-resonant nodeless fibers (DNANF) have shown losses as low as 0.17 dB/km in the C-band [3].

To date, very few irradiation experiments have been conducted on PBGFs [4-7]. These showed RIA character like that of SMFs, but with lower magnitude, as might be expected for structures in which the optical modes propagate mostly in air and has only slight overlap with the glass. ARFs further reduce the fraction of light carried in the glass, and can have values below 100 ppm, which is 10-100x lower than in PBGFs [8]. This suggests ARF radiation performance might further improve over solid core fibers and PBGFs, but to date no studies have been performed on radiation effects in ARFs in the near-infrared, in particular in the C-band. This work aims to assess the RIA in ARF and compare it to radiation resistant single-mode solid-core fibers (RR-SMF). The RR-SMFs studied were fluorine-doped, known to be the most radiation resistant solid core optical fibers in the NIR domain when under continuous irradiation at room temperature [9-10]. The ARFs studied were 5-tube nested anti-resonant nodeless fibers (NANF) [11].

## 2. Experimental Set-up and Method

Two RIA experiments are reported in this paper. Both had the same experimental set-up, but different beam types. In the first experiment (EXP-1), the fibers under test (FUT) were irradiated under  $\gamma$ -rays whereas in the second experiment (EXP-2) the FUTs were irradiated under X-rays. The X-rays are generated by a X-ray tube with a tungsten target operated at 100 kV. The  $\gamma$ -rays are emitted from a <sup>60</sup>Co source and give rise to two peaks at respectively 1.17 MeV and 1.33 MeV. Each experiment had two FUTs: a fluorine-doped RR-SMF whose radiation response has been previously studied [12] and a 5-tube NANF. Those FUTs are denoted as RR-SMF-1 and NANF-1 for EXP-1, as well as RR-SMF-2 and NANF-2 for EXP-2. Note that the fibers were from different preforms. The core diameter of the RR-SMFs was 8.3  $\mu$ m whereas NANF-1 and NANF-2 had respectively 31.9  $\mu$ m and 30.5  $\mu$ m core diameters. A scanning electron microscope image of the cross-section of NANF-2 can be found in Fig. 1.

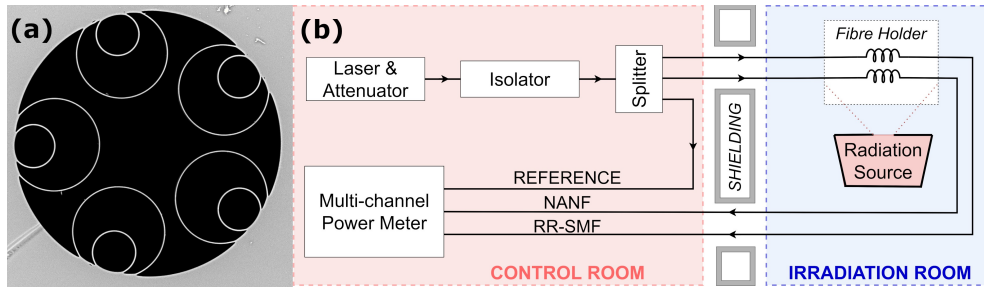


Fig. 1. (a) Scanning electron microscope image of NANF-2. (b) Sketch of the experimental set-up.

A sketch of the set-up is also shown in Fig. 1. The set-up includes two channels for each FUT and a reference channel. The reference channel does not enter the irradiation room and allows monitoring of the optical source intensity. The source is a DFB laser diode centered at 1550 nm with below 1 nm spectral width. InGaAs detectors measured the optical throughput power of each fiber. In both experiments, the NANF ends were directly spliced to pieces of RR-SMFs, which connected them to the light source and detectors. The optical power injected at the FUT was around -11 dBm for the RR-SMFs and -15.5 dBm for the NANFs. This difference is due to the lossy SMF-NANF splices at which there is an inherent mode field profile mismatch. Mode field adaptors can reduce such splices losses but have been avoided, as their radiation response is unknown. The effect of photobleaching with -11 dBm of injected light in the RR-SMFs has shown to be limited [13].

The irradiations were performed at CERN. The dose rate in  $^{60}\text{Co}$   $\gamma$ -rays was measured using an ionization chamber (model PTW 23331) whereas a combination of commercial diode dosimeter and in-house fiber-based dosimeter [14] was used for the X-ray facility. Details about the irradiation conditions of each FUT can be found in Tab. 1 alongside FUT parameters. The RIA is computed by scaling the FUT signal to the baseline powers measured before the irradiation, and by taking into account the reference channel and the length of the considered FUT. Additionally, the temperature and humidity were monitored throughout the experiments.

Table 1. Details of the two irradiation experiments and the corresponding FUT parameters.

	EXP-1 ( $\gamma$ -rays)		EXP-2 (X-rays)	
	RR-SMF-1	NANF-1	RR-SMF-2	NANF-2
<b>Mean Dose Rate (Gy/s)</b>	$0.027 \pm 1.8\%$	$0.025 \pm 2.8\%$	$0.182 \pm 2.6\%$	$0.226 \pm 10.0\%$
<b>Total Ionizing Dose (kGy)</b>	60.9	57.4	255.7	318.3
<b>Irradiation Time (hours)</b>	625.3		391.3	
<b>Detection Limit (dB/km)</b>	0.06	0.12	0.30	0.15
<b>Length (m)</b>	431.0	514.0	84.0	100.0
<b>Fiber Loss at 1550 nm (dB/km)</b>	0.26	1.30	0.26	1.33

### 3. Results

The RIA as a function of the dose for each FUT in EXP-1 and EXP-2, as well as the fiber recovery, are shown in Fig. 2. In both experiments, the NANFs displayed a significantly higher radiation hardness compared to the RR-SMFs. The detection limit of each FUT was computed based on the peak-to-peak value of the high-frequency components of measured intensities in the FUT channel and in the reference channel. The computed values can be found in Tab. 1. In EXP-1, no RIA could be observed in NANF-1 above its 0.12 dB/km detection limit. In EXP-2, during the first 200 kGy of TID, NANF-2 exhibited a slight increase of the RIA up to 0.29 dB/km before stabilizing. On the contrary, RR-SMF-1 and RR-SMF-2 showed a clear attenuation from the start to the end of the irradiation. Moreover, unlike the RR-SMFs, the NANFs did not display any recovery after the stop of the irradiation.

### 4. Discussion

The RIA values are much lower in the NANFs than the RR-SMFs. As NANFs possess low overlap between the optical modes and the silica material, there is minimal interaction between the light and radiation induced defects in the glass microstructure. The RIA trend of the NANFs contrasts starkly with the RIA trend of SMFs, as well as with previously reported RIA curves in PBGFs [4-7]. For instance, the absence of the common sharp exponential growth in the RIA curves of the NANFs can be noticed. This suggests that the limited drift observed in both NANFs is not related to the primary RIA mechanisms known for solid-core silica fibers, but rather a potential ARF-specific effect.

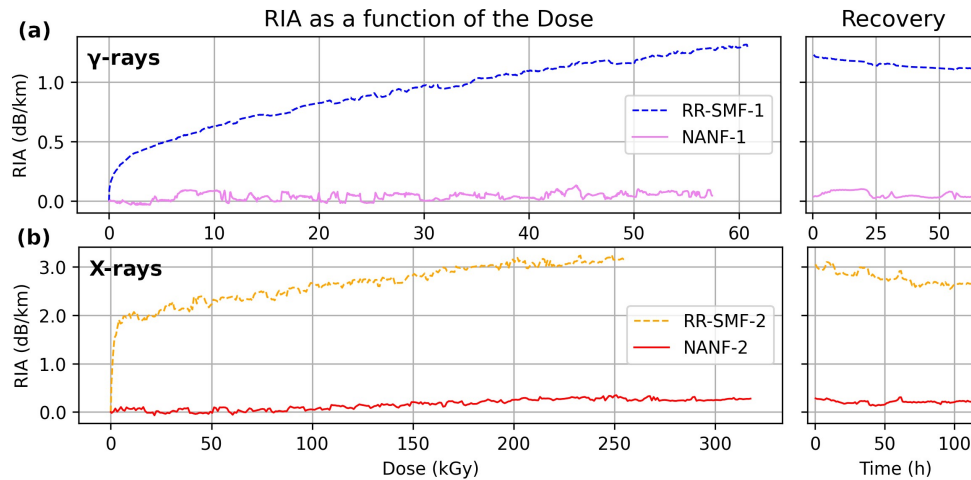


Fig. 2. RIA as a function of the dose for (a) experiment EXP-1 under  $\gamma$ -rays and (b) EXP-2 under X-rays, as well as the FUT recovery after the stop of the irradiation.

Despite the use of relatively long samples, the detection limit of the set-up in EXP-1 was not sufficient to detect any positive RIA in NANF-1. Challenges in measurement accuracy emerge from the extreme radiation hardness of these novel fibers. For instance, the reported 0.29 dB/km RIA in EXP-2 measured using 100 meters of NANF-2, effectively corresponds to a 0.029 dB power difference over 16 days.

## 5. Conclusion

The present research demonstrated for the first time near-zero RIA in NANFs. The radiation resistance of the NANFs measured under both  $\gamma$ -rays and X-rays correspond to the lowest RIA ever observed in optical fibers at 1550 nm under continuous irradiation up to a few hundreds of kGy. These results open new possibilities for the use of NANFs, or their lower loss equivalent the DNANFs, as radiation insensitive fibers in a variety of applications that require operation in radiation environments without any light transmission penalty. Those may include for instance extraterrestrial fiber-based optical communications, high-energy physics experiments, or fiber-based systems that need to operate under extreme radiation conditions, such as in the nuclear industry and at ITER for which those RIA-free fibers might be the only viable solution.

## 4. Acknowledgements

The authors thank Matteo Brucoli, Salvatore Danzeca, Carlos Solans Sanchez, and Konstantin Vidiajev for their help in preparing the experiments and the EPSRC Airguide Photonics (EP/P030181/1) project for support.

## 5. References

- [1] S. Girard et al., "Overview of radiation induced point defects in silica-based optical fibers," *Reviews in Physics* **4**, 100032 (2019).
- [2] S. Girard et al., "Recent advances in radiation-hardened fiber-based technologies for space applications," *J Opt* **20**, 093001 (2018).
- [3] G. T. Jasion, et al. "0.174 dB/km Hollow Core Double Nested Antiresonant Nodeless Fiber (DNANF)," OFC, San Diego, USA, 2022
- [4] H. Henschel et al., "High radiation hardness of a hollow core photonic bandgap fiber," RADECS, Cap d'Agde, France, 2005.
- [5] S. Girard et al., "Radiation-induced effects in a new class of optical waveguides: the air-guiding photonic crystal fibers", *J IEEE Trans Nucl Sci* **52**, 2683–2688 (2005).
- [6] G. Cheymol et al., "High Level Gamma and Neutron Irradiation of Silica Optical Fibers in CEA OSIRIS Nuclear Reactor," *J IEEE Trans Nucl Sci* **55**, 2252–2258 (2008).
- [7] L. Olanterä et al., "Gamma irradiation of minimal latency Hollow-Core Photonic Bandgap Fibers," *Journal of Instrumentation* **8**, C12010–C12010 (2013).
- [8] V. Michaud-Belleau et al., "Backscattering in antiresonant hollow-core Fibers: over 40 dB lower than in standard optical fibers," *Optica* **8**, 216-219 (2021).
- [9] R.E. Youngman et al., "Structural role of fluorine in amorphous silica," *J Non-Cryst Solids* **349**, 10-15 (2004).
- [10] G. Origlio et al., "Irradiation induced defects in fluorine doped silica," *Nucl Instr Methods B* **266**, 2918-2922 (2008).
- [11] F. Poletti, "Nested antiresonant nodeless hollow core fiber," *Optics Express* **22**, 23807-23828 (2014).
- [12] E. Guillermain et al., "Large-Scale Procurement of Radiation Resistant Single-Mode Optical Fibers for CERN," *IEEE J Lightwave Technol* **33**, 4878–4884 (2015).
- [13] T. Wijnands et al., "Optical absorption in commercial single mode optical fibers in a high energy physics radiation field," *J IEEE Trans Nucl Sci* **55**, 2216-2222 (2008).
- [14] D. Di Francesca, et al., "Qualification and Calibration of Single-Mode Phosphosilicate Optical Fiber for Dosimetry at CERN," *IEEE J Lightwave Technol* **37**, 4643–4649 (2019).